HHS Public Access

Author manuscript

Mol Pharm. Author manuscript; available in PMC 2023 May 30.

Published in final edited form as:

Mol Pharm. 2022 November 07; 19(11): 4017–4025. doi:10.1021/acs.molpharmaceut.2c00490.

Development of an In Vitro System To Emulate an In Vivo Subcutaneous Environment: Small Molecule Drug Assessment

Hao Lou,

Department of Pharmaceutical Chemistry and Biopharmaceutical Innovation and Optimization Center, University of Kansas, Lawrence, Kansas 66047, United States

Michael J. Hageman

Department of Pharmaceutical Chemistry and Biopharmaceutical Innovation and Optimization Center, University of Kansas, Lawrence, Kansas 66047, United States

Abstract

A reliable in vitro system can support and guide the development of subcutaneous (SC) drug products. Although several in vitro systems have been developed, they have some limitations, which may hinder them from getting more engaged in SC drug product development. This study sought to develop a novel in vitro system, namely, Emulator of SubCutaneous Absorption and Release (ESCAR), to better emulate the in vivo SC environment and predict the fate of drugs in SC delivery. ESCAR was designed using computer-aided design (CAD) software and fabricated using the three-dimensional (3D) printing technique. ESCAR has a design of two acceptor chambers representing the blood uptake pathway and the lymphatic uptake pathway, respectively, although only the blood uptake pathway was investigated for small molecules in this study. Via conducting a DoE factor screening study using acetaminophen solution, the relationship of the output (drug release from the "SC" chamber to the "blood circulation" chamber) and the input parameters could be modeled using a variety of methods, including polynomial equations, machine learning methods, and Monte Carlo simulation-based methods. The results suggested that the hyaluronic acid (HA) concentration was a critical parameter, whereas the influence of the injection volume and injection position was not substantial. An in vitro–in vivo correlation (IVIVC) study was developed using griseofulvin suspension to explore the feasibility of applying ESCAR in formulation development and bioequivalence studies. The developed LEVEL A IVIVC model demonstrated that the in vivo PK profile could be correlated with the in vitro release profile. Therefore, using this model, for new formulations, only in vitro studies need to be conducted in ESCAR, and in vivo studies might be waived. In conclusion, ESCAR had important implications for research and development and quality control of SC drug products. Future work would be

Corresponding Authors lou0@ku.edu, mhageman@ku.edu.

The authors declare no competing financial interest.

ASSOCIATED CONTENT

Supporting Information

The Supporting Information is available free of charge at https://pubs.acs.org/doi/10.1021/acs.molpharmaceut.2c00490.

Release profiles of the 18 DoE runs using 10 mg/mL acetaminophen solution; release profiles simulated by the Monte Carlo-based methods; prediction profiler plots of release fraction; summary of the goodness of fit of regression models for acetaminophen release profiles; parameters of Weibull function for fitting in vitro release profiles of griseofulvin suspensions; and pictures of the ESCAR setup (PDF)

focused on further optimizing ESCAR and expanding its applications via assessing more types of molecules and formulations.

Graphical Abstract

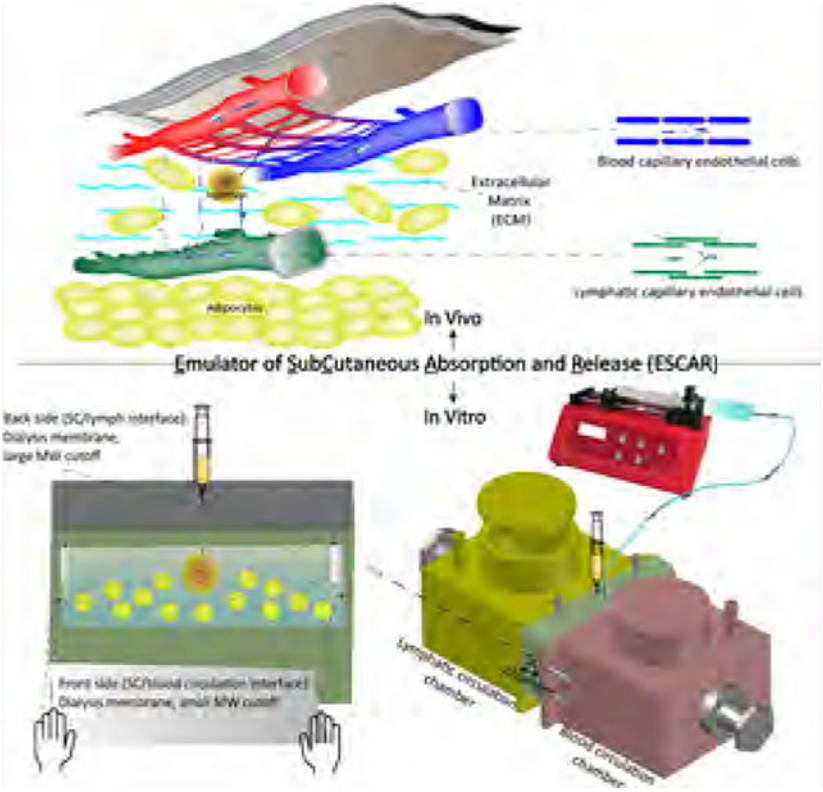

Keywords

subcutaneous route of administration; in vitro system; 3D printing; in vitro–in vivo correlation (IVIVC); machine learning; Monte Carlo simulation; Design of Experiment (DoE)

1. INTRODUCTION

The subcutaneous (SC) route of administration has demonstrated many advantages in delivering a wide variety of therapeutics, for example, small molecules,[1,2] peptides[3–5] proteins,[6–9] and oligonucleotides.[10,11] Also, to enable SC administration and target different sites of action, multiple formulations/drug delivery systems are developed, including highly concentrated solutions, semi-aqueous solutions, non-freeze-dried solid formulations, complexes/clusters, coformulations, suspensions, liposomes, nanoparticles, microparticles, hydrogels, and so forth.[8,9,12–14] Despite many accomplishments, to date, there remain several knowledge gaps regarding drug absorption from the SC injection site, which hamper the accurate prediction of SC bioavailability and other pharmacokinetic (PK) properties such as C_{max} and T_{max}.[15,16] Unfortunately, animal studies may fail to guide human studies because of the lack of translatability for SC delivery between humans and those commonly-

used preclinical species.[17] Compared to in vivo models, in vitro/in silico models generally involve less cost, experimental time, ethical issues, and avoid subject-to-subject variability. Furthermore, in vitro/in silico models would become more attractive if they can predict drug performance in vivo and even present some levels of in vitro–in vivo correlation (IVIVC).

A reliable and robust in vitro system for SC administration would be similar to dissolution apparatus for oral administration. For oral products, USP apparatus 1 (basket) and 2 (paddle) are typically used as a routine method in quality control and as a powerful tool for molecule/formulation development in research and development. In addition, researchers can choose more physiologically relevant systems such as USP apparatus 3 (reciprocating cylinder) and gastro-intestinal simulator (GIS).[18–20] On the contrary, for SC products, currently, there is no standard in vitro system/method/simulated SC medium.[21] Some pioneering research has been conducted to develop new instruments/systems and apply them in SC drug formulation dissolution/release tests. These systems include dispersion releaser (DR), SC injection site simulator (SCISSOR), shake-flask setup, flow-through cell, hydrogel assay in an IVIS system, UV imaging system, and so forth.[21] It is noted that the dispersion releaser (DR), a modification of a USP apparatus 1 via replacing the basket with a vessel, has presented some capabilities in predicting the in vivo performance of SC formulations.[22–24] SCISSOR is the first commercialized instrument that aims to model the SC environment and simulate drug migration from the injection site to the absorption site. Our previous work developed a Monte Carlo method to simulate particle movement inside SCISSOR and identified a list of potential critical parameters.[25] SCISSOR has been successfully applied in some research activities associated with molecule screening, formulation development, and bioavailability prediction.[26–29]

Despite the strengths of DR and SCISSOR, they have some limitations. First, both of them use one donor chamber to represent the SC site and one acceptor chamber to represent the drug uptake. However, for SC administration, there exist two drug uptake pathways: (a) the blood pathway and (b) the lymphatic pathway.[30] Hence, the one-acceptor-chamber design cannot investigate two pathways simultaneously. Second, the geometries of these systems may limit their capability of emulating some biomechanical properties, for example, SC interstitial pressure/convection, transcapillary flux, and so forth.

In this study, a novel in vitro system named Emulator of SubCutaneous Absorption and Release (ESCAR) is developed to assess the SC administration of small molecules (presented in this study) and large molecules (aimed to be presented in our subsequent study). ESCAR has two acceptor chambers, representing the blood pathway and the lymphatic pathway, respectively. However, because the blood pathway is the predominant pathway for small molecule absorption,[7,31] we only focused on drug release to the “blood circulation” chamber in this study. Hyaluronic acid (HA) solution was used to simulate the SC extracellular matrix (ECM). Furthermore, if drug hydrophobicity and adipose tissue/skin lipid were taken into consideration, an O/W emulsion containing lecithin (oil phase) and HA/PBS (aqueous phase) was used as the simulated SC medium. A series of process parameters including HA concentration, injection volume, and injection position (needle tip position) were systemically investigated by a Design-of-Experiment (DoE) study. Furthermore, an IVIVC model was developed based on ESCAR.

2. MATERIALS AND METHODS

2.1. Materials.

ABSplus white and SR-30 were purchased from Stratasys (Edina, MN, USA). Acetaminophen (≥ 99.0%), griseofulvin (97.0–102.0%), and Tween 80 were purchased from Sigma-Aldrich (St.Louis, MO, USA). Lecithin (90%, soybean) and SpectraPor dialysis membranes (50 kDa MWCO regenerated cellulose membranes and 300-kDa MWCO cellulose ester membranes) were purchased from Fisher Scientific (Ward Hill, MA, USA). Hyaluronic acid (average molecular weight: 1.64 M Da) was purchased from Lifecore Biomedical, Inc. (Chaska, MN, USA). All solvents used in this study were HPLC analytical grade.

2.2. ESCAR Design To Emulate the In Vivo SC Environment.

ESCAR aims to have a reasonable emulation of the in vivo SC environment. Inside the human SC site, there is an extensive distribution of blood microcirculation that is mainly organized and controlled by horizontal plexuses at the dermal-SC junctions, as well as many capillaries extending into deep adipose tissue.[32,33] On the contrary, there is less distribution of lymphatic vessels, which are mainly large lymphatic vessels but are seldom microcirculatory lymphatic vessels.[34,35]

Lymphatic capillaries are more “open” compared to blood capillaries. The outer walls of the lymphatic capillaries are composed of a single layer of loosely adherent and overlapped endothelial cells. The “cleft-like” intercellular junctions (junction size: in the range of 15 and 100 nm to even several microns) allow fluid as well as macromolecules/colloids in the fluid to freely enter the lymphatics.[15,31,36,37] Unlike lymphatic capillary walls, tight inter-endothelial junctions (e.g., adherens junctions and tight junctions) are present on blood capillary walls, which restrict the paracellular transport of molecules with a size larger than 3 nm, although some macromolecules such as albumin, hormones, insulin, and so forth can still cross endothelial cells via transcellular or transcytotic pathways.[15,31,36–38] Previous studies reported that a series of proteins followed a trend that the extent of lymphatic uptake increased with molecular weight, for example, insulin (MW: 5.8 kDa),[39] cytochrome c (MW: 12.3 kDa),[40] human growth hormone (MW: 22 kDa),[41] rHuEPO (MW: 30.4 kDa),[42] and darbepoetin alfa (MW: 37.0 kDa).[43,44] In a nutshell, blood uptake is the primary pathway for small molecules, and lymphatic uptake plays an important role in absorbing large molecules. There also exists convection inside the SC space, which, according to the Starling theory, is driven by the capillary hydrostatic pressure between the arteriole and interstitium, as well as the interstitial colloid osmotic pressure.[45,46] The flow rate from the interstitium into the lymphatic system typically ranges from 0.2 to 1 μm/s.[47] The migration of large molecules inside the SC ECM is significantly impacted by convection, while the migration of small molecules is mainly controlled by diffusion.[7]

As shown in Figure 1, ESCAR consists of three compartments: the “SC” chamber, the “blood circulation” chamber, and the “lymphatic circulation” chamber. The three chambers can be tightened by adjusting knobs or clamps. The “SC” chamber, representing the SC site, is a rectangular cuboid with two open surfaces at the front and back sides. The top side

of the “SC” chamber has either a ceiling that is integrated into the whole chamber or an open-framed window that can be sealed by a membrane (e.g., Parafilm M membrane). Also, there are two versions of the “SC” chamber, as shown in Figure 1.

For the “SC” chamber (Version 1), the open surfaces at the front and back sides represent two drug uptake pathways: (a) the blood pathway and (b) the lymphatic pathway. The “SC” chamber (Version 1) has a total volume of around 2.8 mL and is designed to reflect the unequal distribution of blood/lymphatic capillaries: (a) the SC/blood circulation interface (the front side) has an open surface of 3 cm^2 surface area (3 cm in length × 1 cm in height), and (b) the SC/lymphatic circulation interface (the back side) has a 2 mm thickness slab covering the central area, and two open slits with 0.1 cm^2 surface area (0.1 cm in length × 1 cm in height) at the left and right ends. Therefore, “blood” uptake has a larger surface area and a shorter distance from the injection site compared to “lymphatic” uptake. Notably, the ratio of these surface areas may need further adjustment, guided by physiological data. The “SC” chamber (Version 1) is designed primarily to test small molecules with a focus on blood absorption. However, to evaluate large molecules, a larger surface area at the back side may be needed to obtain faster drug release and shorter experimental time.

The “SC”/“lymphatic circulation” interface is covered by a membrane with large pores representing the open intercellular gaps of lymphatic capillaries. For instance, a SpectraPor dialysis membrane with 300 kDa MWCO was used in this study, but larger pores may be used for future studies. On the other hand, blood capillaries have tight inter-endothelial junctions. Therefore, at the “SC”/“blood circulation” interface, a SpectraPor dialysis membrane with 50 kDa MWCO is installed to represent “blood” uptake. To emulate the infinite sink condition after drug uptake, both the “blood circulation” and the “lymphatic circulation” chambers are larger than 75 mL, at least 20 orders of magnitude to the volume of the “SC” chamber. In addition, we aim to emulate the unidirectional fluid flow through SC interstitium to lymphatic capillaries in vivo. In ESCAR, convection can be generated by feeding a liquid flow into the “SC” chamber using a syringe pump. The impact of convection would be presented in our subsequent paper.

The “SC” chamber (Version 2) is designed to represent the SC sites of rats. It was reported that for rats, the extent of lymphatic uptake was low for small molecules, and even for some large molecules;[48] therefore, both sides of the “SC” chamber represent “blood” uptake. Compared to Version 1, Version 2 has a larger chamber volume (~7.5 mL) and larger interfacial surfaces (7.5 cm^2 × 2) because rats have more loose SC connective tissue compared to humans, and injected formulation would spread more widely and rapidly in rats’ SC site.[17] Some pictures of the ESCAR setup are presented in Figure S4 in the Supporting Information.

2.3. ESCAR Fabrication.

The ESCAR layout was drawn using AutoCAD (Autodesk Inc., San Rafael, CA, USA). Each component was printed using a Mojo 3D printer (Stratasys, Inc., Edina, MN, USA) via the fused deposition modeling technology. ABSplus white (an acrylonitrile butadiene styrene-based thermoplastic material) and SR-30 were utilized as the printing material and the support material, respectively. After printing, the support material was removed by the

Ecoworks-based solution with the aid of a WaveWash 55 Clean system (Stratasys, Inc., Edina, MN, USA). Acetone was sprayed onto the outer and inner surfaces to make the components watertight. Sequentially, the acetone-treated components were placed under (i) ambient temperature overnight and then (ii) at 50 °C in a convection oven for at least 72 h to remove the acetone residues. Furthermore, all the contact surfaces were smoothened by a series of sandpapers with medium grits and superfine grits.

2.4. Drug Quantification Using HPLC.

A Shimadzu HPLC system (Shimadzu Corporation, Kyoto, Japan) equipped with an XBridge C18 column (3.5 μM, 4.6 × 150 mm) was used to quantify the acetaminophen and griseofulvin samples.

For acetaminophen samples, 20 μL was injected and detected at 275 nm. The mobile phase containing 69% of water, 3% of acetic acid, and 28% of methanol (v/v) was kept at a constant flow rate of 0.8 mL/min. The column chamber temperature was set at 27 °C and the detector chamber temperature was maintained at 40 °C. For griseofulvin samples, 20 μL was injected and detected at 291 nm. The mobile phase containing 35% of water with 0.1% of trifluoroacetic acid and 65% of acetonitrile (v/v) was kept at a constant flow rate of 1 mL/min. The temperature of both the column chamber and the detector chamber was kept at 40 °C.

2.5. ESCAR Drug Binding/Adsorption Study.

ESCAR drug binding/adsorption study was carried out using a procedure as follows: 75 mL of acetaminophen or griseofulvin solution with a known concentration was placed in an ESCAR's acceptor chamber, and the chamber was stored at ambient temperature for 24 h before the sample collection. The measurements were carried out in triplicate. The percentage of drug recovery was calculated using eq 1.

$$\text{Recovery}(\%) = \frac{\text{Concentration (after 24 h in chamber)}}{\text{Concentration (initial)}} \times 100\% \quad (1)$$

2.6. DoE Factor Screening Study Using Acetaminophen Solution.

2.6.1. Drug Release Tests for Acetaminophen.—Acetaminophen solution (10 mg/mL) and the "SC" chamber (version 1) were used across different runs. Both the "lymphatic circulation" and "blood circulation" chambers were filled with 75 mL of PBS (pH 7.4), and the "SC" chamber was filled with 2.8 mL of HA/PBS solution. At the surrounding areas of the interfaces, a layer of mounting tape was assembled to prevent liquid leakage. Sequentially, the "SC"/"blood circulation" interface was assembled with a SpectraPor dialysis membrane (MWCO: 50 kDa), and the "SC"/"lymphatic circulation" interface was assembled with a SpectraPor dialysis membrane (MWCO: 300 kDa). All membranes were presoaked in DI water for at least 1 h before use. The drug release tests were conducted at 34 °C in a convective oven, with mild magnetic stirring in the "blood circulation" and "lymphatic circulation" chambers. Notably, no stirring was applied in the "SC" chamber. The preset volume of the drug solution was manually injected into the "SC" chamber from the injection port(s) using a 3 mL syringe connected with a 23G × 3/4 needle

(BD, Franklin Lakes, NJ, USA). An 18 run full factorial experimental design was employed to evaluate three factors, HA concentration (three levels: 2.5, 5, and 10 mg/mL because this concentration range was commonly used in previous studies[26–29,49,50]), injection volume (three levels: 0.25, 0.5, and 1 mL), and injection position/needle tip position to the membrane at the "SC"/"blood circulation" interface (two levels: 0.2, 0.5 cm). At the preset time points, 1.5 mL of aliquots were withdrawn from the "blood circulation" chamber with the replacement of the same volume of PBS. Each run was conducted in triplicate. Our preliminary study found that drug concentration in the "lymphatic circulation" chamber was around 40–50 times less than that in the "blood circulation" chamber. Therefore, in the present study, drug release to the "lymphatic circulation" chamber was not analyzed.

2.6.2. Release Profile Modeling Using Statistical and Machine Learning Methods.—

A series of statistical and machine learning methods were adopted to model the relationship between the input factors and the output response(s) based on the data generated from the 18-run DoE study. The HA concentration (X_1), injection volume (X_2), and injection position to the membrane (X_3) were three input factors. Release percentages (Y) at 2, 4, 6, and 8 h were selected as the output response(s).

For statistical methods, the data were fit by polynomial equations with the aid of JMP (SAS Institute, Cary, NC, USA). After removing some statistically insignificant second-order and interaction terms, the final format of the polynomial equations was expressed as eq 2.

$$Y = \text{intercept} + aX_1^2 + bX_1 + cX_2 + dX_3 \quad (2)$$

A total of four machine learning methods, including support vector machine (SVM), random forest (RF), gradient boosting, and multilayer perceptron (MLP), were also used to develop regression models. The codes were programmed based on the Scikit-Learn module under the Python environment, and hyperparameters were tuned using the cross-validated grid search method.[51]

The release data could also be simulated by the Monte Carlo simulation-based methods. The relevant procedure is provided in the Supporting Information.

2.7. IVIVC Development for Griseofulvin Suspensions.

2.7.1. In Vivo Data Collection.—

Chiang et al. developed a series of un-milled and milled suspensions for SC administration and conducted rat PK studies.[52] The data of the average plasma concentration of griseofulvin from 0 to 24 h were extracted from Figure 6 in their study using Origin 2018 (OriginLab Corporation, Northampton, MA, USA).[52]

2.7.2. Griseofulvin Suspension Preparation.—

Referring to Chiang et al., the same vendor of the bulk griseofulvin powder and similar preparation methods were used in the present study.[52] Briefly, to prepare the un-milled suspension, the predetermined amount of bulk powder was dispensed in 0.5% Tween 80 (w/w) PBS solution, followed by a 5 min sonication. The un-milled suspension was characterized using a Mastersizer 3000 particle size analyzer (Malvern Panalytical, Westborough, MA, USA). To prepare the

milled suspension, bulk griseofulvin powder and 0.5 mm zirconium beads were added to a scintillation vial, followed by the addition of 0.5% Tween 80 (w/w) PBS solution to obtain a final concentration of 50 mg/mL. The suspension was wet-milled under magnetic stirring at 1200 rpm with occasional shaking for 24 h. The particle size of the milled suspension was characterized using a Zetasizer (Malvern Panalytical, Westborough, MA, USA) instrument.

2.7.3. In Vitro ESCAR Drug Release Tests for Griseofulvin.—The "SC" chamber (version 2) was used for the in vitro release tests of griseofulvin un-milled and milled suspensions. For this chamber design, both the front and back interfaces were in contact with the "blood circulation" chambers filled with 75 mL of PBS (pH 7.4), and each interface was assembled with a SpectraPor dialysis membrane (MWCO: 50 kDa). Furthermore, in the surrounding areas of the interfaces, a layer of mounting tape was assembled to prevent liquid leakage. The "SC" chamber was filled with 7.5 mL of the O/W emulsion composed of 1.64% (w/v) lecithin and 1 mg/mL HA in PBS solution. The formulation, dose, and injection volume of our in vitro studies were equivalent to those used in the in vivo studies.[52] In the in vivo study, the rat body weight ranged from 300 to 350 g. To maintain the consistency of the dose for our in vitro study, 300 g was selected for in vitro–in vivo conversion. For example, if the in vivo dose was 30 mg/kg, the dose of the in vitro release tests was 9 mg. The suspension was injected from the injection port at the center using a 3 mL syringe connected with a 23G × 3/4 needle (BD, Franklin Lakes, NJ, USA), and the release test was undertaken at 34 °C with mild magnetic stirring inside the "blood circulation" chambers. Notably, no stirring was applied in the "SC" chamber. For the sampling points before 8 h, 1.5 mL of aliquots (0.75 mL from each "blood circulation" chamber) were withdrawn with the replacement of PBS; and for the sampling points at 8 h and beyond, to maintain the concentration gradient between the "SC" chamber and the "blood circulation" chambers and prevent the solution in the "blood circulation" chamber from saturation, 100 mL of aliquots (50 mL from each "blood circulation" chamber) were withdrawn with the replacement of PBS. Each trial was undertaken in triplicate. The release profiles were fit using a three-parameter Weibull equation, expressed as eq 3.

$$Y = a \times \left(1 - \exp\left(-\left(\frac{t^b}{c}\right)\right)\right) \tag{3}$$

where Y is release fraction (%), t is time, and a, b, and c are three constants that could be obtained by curve fitting.

2.7.4. One-Step LEVEL A IVIVC Model.—Griseofulvin's rat PK profiles could be fit using a two-compartment model.[52] The mathematical equations corresponding to the change of drug amounts in the central and peripheral compartments (shown in Figure 3b) were described by eqs 4–6.

$$\frac{dAmt1}{dt} = Abs.\ Rate\ - k_{10}Amt1 - k_{12}Amt1 + k_{21}Amt2 \tag{4}$$

$$\frac{dAmt2}{dt} = k_{12}Amt1 - k_{21}Amt2 \tag{5}$$

$$Conc1 = \frac{Amt1}{V_c} \tag{6}$$

where $Amt1$ and $Amt2$ are the drug amounts in the central and peripheral compartments at time t, $Conc1$ is the plasma concentration at time t, V_c is the volume of distribution in the central compartment, k_{10}, k_{12}, and k_{21} are the rate constants for elimination, transfer from the central to the peripheral, and transfer from the peripheral to the central, respectively. The values of V_c, k_{10}, k_{12}, and k_{21} were calculated and reported by Chiang et al.[52] *Abs. Rate*, the in vivo absorption rate from the SC site at time t, was defined and hypothesized to be correlated to the in vitro release rate using a quadratic equation, as expressed by eq 7.

$$\begin{aligned} Abs.\ Rate &= \{[\ Dose \times F(t+\Delta t|_{\text{in vivo}}) - \ Dose \times F(t|_{\text{in vivo}})] \\ &/[\Delta t|_{\text{in vivo}}]\} = \{[\ Dose \times F(b_0 + b_1 \times (t+\Delta t) \\ &+ b_2 \times (t+\Delta t)^2{}_{\text{in vitro}}) - \ Dose \times F(b_0 + b_1 \times t \\ &+ b_2 \times t^2|_{\text{in vitro}})]/[b_0 + b_1 \times (t+\Delta t) \\ &+ b_2 \times (t+\Delta t)^2|_{\text{in vitro}} - b_0 + b_1 \times t + b_2 \times t^2|_{\text{in vitro}}]\} \end{aligned} \tag{7}$$

where F is the percentage of the drug absorbed (in vivo) or the percentage of drug released (in vitro) at time t, and b_0, b_1, and b_2 are time-scaling factors for IVIVC. By tuning b_0, b_1, and b_2, the model that had the best fit of the plasma concentration could be obtained by numerically solving eqs 4–6, using the custom codes programmed in Matlab R2018a (MathWorks, Natick, MA, USA).

3. RESULTS AND DISCUSSION

3.1. Drug Binding/Adsorption to ESCAR.

Drug binding/adsorption to the device (e.g., ESCAR) would interfere drug content in the medium. ESCAR was assessed using two small molecule drugs: acetaminophen and griseofulvin. After 24 h, the recovery (%) of (i) acetaminophen was 99.6 ± 0.2%, and that of (ii) griseofulvin was 95.5 ± 1.7%. Hence, both drugs had limited drug binding/adsorption to ESCAR. Furthermore, acetaminophen had a slightly higher recovery (%), which might be because acetaminophen was more hydrophilic compared to griseofulvin.

3.2. ESCAR Factor Screening Study Using Acetaminophen Solution.

Acetaminophen solution was used to evaluate ESCAR and identify critical parameters for drug release. HA-containing buffered solutions were widely used as simulated SC media for in vitro release tests of hydrophilic molecules.[26–29,49,50] The impact of three factors (HA concentration, injection volume, and injection position to the membrane at the “SC”/“blood circulation” interface) on drug release was studied via an 18-run full factorial study. As shown in Figure 2a, the increase in the HA concentration slowed the drug release, for

example, for the center position injection, the release fraction (%) values were (i) ~30% at 2 h and ~60% at 8 h in 2.5 mg/mL HA solution; (ii) ~10% at 2 h and ~30% at 8 h in 5 mg/mL HA solution; (iii) ~5% at 2 h and ~15% at 8 h in 10 mg/mL HA solution. The complete results of the release profiles are presented in Figure S1 in the Supporting Information. From the molecular-level perspective, drug release from the "SC" chamber consisted of two steps: (i) drug molecules migrated from the position after the injection to the absorption site (membrane) and then (ii) molecules penetrated through the membrane to the acceptor chamber. The release data indicated that using high HA solutions (e.g., 5 and 10 mg/mL), drug release was predominantly controlled by drug migration from the injection site to the absorption site, whereas using PBS or low HA solutions (e.g., 2.5 mg/mL), drug molecules diffused faster in the medium, and drug penetration through the membrane should have more impact on drug release.

A series of statistical and machine learning methods were developed to model the relationship between the input factors and the output response (drug release). The DoE study data were used for model training and validation. As seen in Figure 2b, the release fraction (%) at different time points (e.g., 2 h) versus three input factors could be fit using polynomial equations (in the format of eq 2) with acceptable fitness. The prediction profiler plots in Figure 2b suggested that the release fraction underwent a rapid decline as the HA concentration increased from 2.5 to 6 mg/mL, and then gradually leveled out while the HA concentration increased above 6 mg/mL. Conversely, the release fraction was not substantially changed by the injection volume and injection position to the membrane. The prediction profiler plots of more timepoints (e.g., 4, 6, and 8 h) are presented in Figure S2 in the Supporting Information.

Unlike the statistical models that require manually set rules and instructions, for example, assigning a second-order polynomial to depict the curvature of the response surface, machine learning methods could learn the data on their own and develop a model(s) with better predictability, although simultaneously, the model interpretability might be compromised. As seen in Table S1 in the Supporting Information, all machine learning models (SVM, RF, gradient boosting, and MLP) presented slightly higher R^2-score values than polynomial equations, suggesting that the training data could be fit better by the machine learning models. To avoid the potential overfitting issue, a 4-fold cross-validation method was developed, where 75% of the data in the whole dataset were used for model training, and the remaining 25% was used for model validation. For this small and simple dataset, all developed statistical and machine learning methods provided good predictions. However, machine learning models should be more capable of handling large datasets with convoluted data patterns and making accurate predictions.

Drug release profiles could also be simulated using the Monte Carlo-based methods. The results are presented in the Supporting Information.

3.3. IVIVC for Griseofulvin Suspensions.

It is of value to explore ESCAR's capability in predicting in vivo PK properties and developing IVIVC models. Our in-house-made un-milled and milled suspensions had similar particle sizes as the suspensions manufactured by Chiang et al., for example, D50 of

the un-milled suspension: 26.2 ± 2.06 μm vs 21.9 μm;[52] D50 of the milled suspension: 1.5 ± 0.2 μm vs 1.7 μm.[52] To date, a wide variety of simulated SC media have been developed.[21] As pointed out by Li et al., a more physiologically relevant medium may not fit the purposes (e.g., IVIVC, QC release, formulation/compound screening, etc.) better; instead, a fit-for-purpose medium must have a good balance of sensitivity, selectivity, and biorelevance.[21] Griseofulvin (clogP: 2.2) is lipophilic and has a higher partition into the oil phase compared to the aqueous phase. To consider the effect of molecule lipophilicity, lecithin was added in the simulated SC medium to represent the potential drug depots such as adipose tissue and skin lipid. Lipophilic drugs (e.g., griseofulvin) can distribute to both the oil phase (dispersed) and the aqueous phase (continuous) and have a distribution volume larger than the apparent volume of the "SC" chamber. On the contrary, lecithin should have minor impact on hydrophilic drugs (e.g., acetaminophen) because hydrophilic molecules preferably distribute in the aqueous phase. Furthermore, because rats' SC space is less dense and less viscous compared to humans' SC space, the low HA level (1 mg/mL) was added in the medium. To attain a release profile for a suspension in ESCAR, drug molecules needed to first dissolve and then the molecules migrated to the membrane, followed by the penetration through the membrane to the acceptor chamber. We speculated that, using this medium, the rate-limiting step of drug release should be the step of particle dissolution rather than the step of molecule diffusion in the medium. The in vitro drug release amount (mg) versus time is presented in Figure 3a. As seen, the milled suspension released faster than the un-milled suspension, for example, given a 9 mg dose, at 102 h, 1.34 mg (amount released of the milled suspension) was 50% higher than 0.89 mg (amount released of the un-milled suspension), indicating the advantage of the micronization on dissolution rate enhancement. Furthermore, the 1.5 mg dose of the milled suspension provided a slightly faster release than the 9-mg dose of the un-milled suspension. While the dose of the milled suspension increased from 9 to 18 mg, the drug release amount enhanced marginally. Another finding was that the in vitro release in ESCAR was slower than the in vivo dissolution/absorption. For instance, according to the data presented in Chiang et al.'s study (Figure 5), for the 9 mg dose of the un-milled suspension, the in vivo drug absorption amount at 24 h was similar to the in vitro drug release amount at 54 h.

To build the IVIVC model, three dose/formulation combinations (9 mg/un-milled, 9 mg/milled, and 18 mg/milled) were used as the internal-validation data, and the in vitro release profiles (%) are plotted in Figure 3c. The high R^2-score values, listed in Table S2 in the Supporting Information, suggested that the release profile (%) could be fit by the Weibull function (eq 3). As presented in Figure 3d, a LEVEL A IVIVC model was developed. Table 1 listed the values of C_{max}, $AUC_{0–24h}$, and the prediction error (%PE). As a result, the model passed the internal validation, and the average absolute internal %PE for C_{max} was 3.6% and that for $AUC_{0–24h}$ was 2.9%. In addition, to make the model more conclusive, the 1.5 mg dose of the milled suspension was evaluated as the external validation. The %PE values for C_{max} and $AUC_{0–24h}$ were 14.9 and −11.5%, respectively. Using this IVIVC model, for a new griseofulvin suspension formulation, only in vitro release tests would need to be conducted in ESCAR, and costly and time-consuming in vivo studies might be waived. Therefore, with this strategy, the 3R (reduce/refine/replace) principle for preclinical species was implemented. Promisingly, using the same methodology, it was also possible to develop

an IVIVC model based on human PK data and apply it to various studies such as new formulation development and bioequivalence studies.

4. CONCLUSIONS

In this study, a prototype of an in vitro system ESCAR was developed to emulate the in vivo SC environment. ESCAR showed its potential uses in the assessment of different SC formulations (e.g., solution and suspension) and small molecule drugs (e.g., hydrophilic molecule: acetaminophen; hydrophobic molecule: griseofulvin). From a factor screening study, it was found that drug release from the "SC" chamber was significantly affected by the HA concentration rather than the injection volume and the injection position. Last but not least, an IVIVC model was successfully developed for griseofulvin suspensions. This established IVIVC model demonstrated that ESCAR had important implications in SC drug product development and bioequivalence studies.

Supplementary Material

Refer to Web version on PubMed Central for supplementary material.

ACKNOWLEDGMENTS

The authors thank Mr. Ryan Grigsby and Dr. Susan Lunte for their support and useful discussion. The authors thank KU Nanofabrication Facility for providing the necessary resources. The authors also thank the support from NIH P20GM103638.

REFERENCES

(1). Hernández-Ruiz V; Forestier E; Gavazzi G; Ferry T; Grégoire N; Breilh D; et al. Subcutaneous Antibiotic Therapy: The Why, How, Which Drugs and When. J. Am. Med. Dir. Assoc. 2021, 22, 50.e6–55.e6. [PubMed: 32674952]

(2). Neklesa TK; Winkler JD; Crews CM Targeted protein degradation by PROTACs. Pharmacol. Ther. 2017, 174, 138–144. [PubMed: 28223226]

(3). Kumar A Insulin degludec/liraglutide: innovation-driven combination for advancement in diabetes therapy. Expert Opin. Biol. Ther. 2014, 14, 869–878. [PubMed: 24702171]

(4). Guo Y; Lei K; Tang L Neoantigen Vaccine Delivery for Personalized Anticancer Immunotherapy. Front. Immunol. 2018, 9, 1499. [PubMed: 30013560]

(5). Sahin U; Türeci Ö Personalized vaccines for cancer immunotherapy. Science 2018, 359, 1355–1360. [PubMed: 29567706]

(6). Kinnunen HM; Mrsny RJ Improving the outcomes of biopharmaceutical delivery via the subcutaneous route by understanding the chemical, physical and physiological properties of the subcutaneous injection site. J. Controlled Release 2014, 182, 22–32.

(7). Viola M; Sequeira J; Seiça, R.; Veiga, F.; Serra, J.; Santos, A. C.; et al. Subcutaneous delivery of monoclonal antibodies: How do we get there? J. Controlled Release 2018, 286, 301–314.

(8). Wang W Advanced protein formulations. Protein Sci. 2015, 24, 1031–1039. [PubMed: 25858529]

(9). Lou H; Feng M; Hageman MJ Advanced Formulations/Drug Delivery Systems for Subcutaneous Delivery of Protein-Based Biotherapeutics. J. Pharm. Sci. 2022, 2968. [PubMed: 36058255]

(10). Davies N; Hovdal D; Edmunds N; Nordberg P; Dahlén A; Dabkowska A; et al. Functionalized lipid nanoparticles for subcutaneous administration of mRNA to achieve systemic exposures of a therapeutic protein. Mol. Ther.–Nucleic Acids 2021, 24, 369–384. [PubMed: 33868782]

(11). Pardi N; Hogan MJ; Porter FW; Weissman D mRNA vaccines — a new era in vaccinology. Nat. Rev. Drug Discovery 2018, 17, 261–279. [PubMed: 29326426]

(12). Marschall C; Witt M; Hauptmeier B; Friess W Powder suspensions in non-aqueous vehicles for delivery of therapeutic proteins. Eur. J. Pharm. Biopharm. 2021, 161, 37–49. [PubMed: 33548460]

(13). Li J; Mooney DJ Designing hydrogels for controlled drug delivery. Nat. Rev. Mater. 2016, 1, 16071. [PubMed: 29657852]

(14). Cai S; Yang Q; Bagby TR; Forrest ML Lymphatic drug delivery using engineered liposomes and solid lipid nanoparticles. Adv. Drug Delivery Rev. 2011, 63, 901–908.

(15). Richter WF; Jacobsen B Subcutaneous Absorption of Biotherapeutics: Knowns and Unknowns. Drug Metab. Dispos. 2014, 42, 1881–1889. [PubMed: 25100673]

(16). Collins DS; Sánchez-Félix M; Badkar AV; Mrsny R Accelerating the development of novel technologies and tools for the subcutaneous delivery of biotherapeutics. J. Controlled Release 2020, 321, 475–482.

(17). Turner MR; Balu-Iyer SV Challenges and Opportunities for the Subcutaneous Delivery of Therapeutic Proteins. J. Pharm. Sci. 2018, 107, 1247–1260. [PubMed: 29336981]

(18). Azarmi S; Roa W; Löbenberg R Current perspectives in dissolution testing of conventional and novel dosage forms. Int. J. Pharm. 2007, 328, 12–21. [PubMed: 17084051]

(19). Hens B; Bermejo M; Tsume Y; Gonzalez-Alvarez I; Ruan H; Matsui K; et al. Evaluation and optimized selection of supersaturating drug delivery systems of posaconazole (BCS class 2b) in the gastrointestinal simulator (GIS): An in vitro-in silico-in vivo approach. Eur. J. Pharm. Sci. 2018, 115, 258–269.

(20). Hens B; Bermejo M; Augustijns P; Cristofoletti R; Amidon GE; Amidon GL Application of the Gastrointestinal Simulator (GIS) Coupled with In Silico Modeling to Measure the Impact of Coca-Cola® on the Luminal and Systemic Behavior of Loratadine (BCS Class 2b). Pharmaceutics. 2020, 12, 566. [PubMed: 32570975]

(21). Li D; Chow PY; Lin TP; Cheow C; Li Z; Wacker MG Simulate SubQ: The Methods and the Media. J. Pharm. Sci. 2021, DOI: 10.1016/j.xphs.2021.10.031.

(22). Janas C; Mast M-P; Kirsamer L; Angioni C; Gao F; Mäntele W; et al. The dispersion releaser technology is an effective method for testing drug release from nanosized drug carriers. Eur. J. Pharm. Biopharm. 2017, 115, 73–83. [PubMed: 28213179]

(23). Gao GF; Ashtikar M; Kojima R; Yoshida T; Kaihara M; Tajiri T; et al. Predicting drug release and degradation kinetics of long-acting microsphere formulations of tacrolimus for subcutaneous injection. J. Controlled Release 2021, 329, 372–384.

(24). Gao GF; Thurn M; Wendt B; Parnham MJ; Wacker MG A sensitive in vitro performance assay reveals the in vivo drug release mechanisms of long-acting medroxyprogesterone acetate microparticles. Int. J. Pharm. 2020, 586, No. 119540. [PubMed: 32590096]

(25). Lou H; Berkland C; Hageman MJ Simulating particle movement inside subcutaneous injection site simulator (SCISSOR) using Monte-Carlo method. Int. J. Pharm. 2021, 605, No. 120824. [PubMed: 34171429]

(26). Kinnunen HM; Sharma V; Contreras-Rojas LR; Yu Y; Alleman C; Sreedhara A; et al. A novel in vitro method to model the fate of subcutaneously administered biopharmaceuticals and associated formulation components. J. Controlled Release 2015, 214, 94–102.

(27). Bown HK; Bonn C; Yohe S; Yadav DB; Patapoff TW; Daugherty A; et al. In vitro model for predicting bioavailability of subcutaneously injected monoclonal antibodies. J. Controlled Release 2018, 273, 13–20.

(28). Shan L; Mody N; Sormani P; Rosenthal KL; Damschroder MM; Esfandiary R Developability Assessment of Engineered Monoclonal Antibody Variants with a Complex Self-Association Behavior Using Complementary Analytical and in Silico Tools. Mol. Pharmaceutics 2018, 15, 5697–5710.

(29). Thati S; McCallum M; Xu Y; Zheng M; Chen Z; Dai J; et al. Novel Applications of an In Vitro Injection Model System to Study Bioperformance: Case Studies with Different Drug Modalities. J. Pharm. Innovation 2020, 15, 268–280.

(30). Kagan L Pharmacokinetic Modeling of the Subcutaneous Absorption of Therapeutic Proteins. Drug Metab. Dispos. 2014, 42, 1890–1905. [PubMed: 25122564]

(31). McLennan DN; Porter CJH; Charman SA Subcutaneous drug delivery and the role of the lymphatics. Drug Discovery Today: Technol 2005, 2, 89–96.

(32). Braverman IM The Cutaneous Microcirculation. J. Invest. Dermatol. Symp. Proc. 2000, 5, 3–9.

(33). Frayn KN; Karpe F Regulation of human subcutaneous adipose tissue blood flow. Int. J. Obes. 2014, 38, 1019–1026.

(34). Redondo P. d. A. G.; Gubert F.; Zaverucha-do-Valle C; Dutra TPP; Ayres-Silva J. d. P.; Fernandes N; et al. Lymphatic vessels in human adipose tissue. Cell Tissue Res. 2020, 379, 511–520. [PubMed: 31776824]

(35). Skobe M; Detmar M Structure, Function, and Molecular Control of the Skin Lymphatic System. J. Invest. Dermatol. Symp. Proc. 2000, 5, 14–19.

(36). Porter CJH; Edwards GA; Charman SA Lymphatic transport of proteins after s. c. injection: implications of animal model selection. Adv. Drug Delivery Rev. 2001, 50, 157–171.

(37). Porter CJH; Charman SA Lymphatic Transport of Proteins After Subcutaneous Administration. J. Pharm. Sci. 2000, 89, 297–310. [PubMed: 10707011]

(38). Komarova Y; Malik AB Regulation of Endothelial Permeability via Paracellular and Transcellular Transport Pathways. Annu. Rev. Physiol. 2010, 72, 463–493. [PubMed: 20148685]

(39). Charman SA; McLennan DN; Edwards GA; Porter CJH Lymphatic Absorption Is a Significant Contributor to the Subcutaneous Bioavailability of Insulin in a Sheep Model. Pharm. Res. 2001, 18, 1620–1626. [PubMed: 11758772]

(40). Supersaxo A; Hein WR; Steffen H Effect of Molecular Weight on the Lymphatic Absorption of Water-Soluble Compounds Following Subcutaneous Administration. Pharm. Res. 1990, 7, 167–169. [PubMed: 2137911]

(41). Charman SA; Segrave AM; Edwards GA; Porter CJH Systemic Availability and Lymphatic Transport of Human Growth Hormone Administered by Subcutaneous Injection. J. Pharm. Sci. 2000, 89, 168–177. [PubMed: 10688746]

(42). McLennan DN; Porter CJH; Edwards GA; Martin SW; Heatherington AC; Charman SA Lymphatic Absorption Is the Primary Contributor to the Systemic Availability of Epoetin Alfa following Subcutaneous Administration to Sheep. J. Pharmacol. Exp. Ther. 2005, 313, 345–351. [PubMed: 15579493]

(43). McLennan DN; Porter CJH; Edwards GA; Heatherington AC; Martin SW; Charman SA The Absorption of Darbepoetin Alfa Occurs Predominantly via the Lymphatics Following Subcutaneous Administration to Sheep. Pharm. Res. 2006, 23, 2060–2066. [PubMed: 16951999]

(44). Kota J; Machavaram KK; McLennan DN; Edwards GA; Porter CJH; Charman SA Lymphatic Absorption of Subcutaneously Administered Proteins: Influence of Different Injection Sites on the Absorption of Darbepoetin Alfa Using a Sheep Model. Drug Metab. Dispos. 2007, 35, 2211–2217. [PubMed: 17875672]

(45). Sawdon M; Kirkman E Capillary dynamics and the interstitial fluid–lymphatic system. Anaesth. Intensive Care Med. 2017, 18, 309–315.

(46). Haggerty A; Nirmalan M Capillary dynamics, interstitial fluid and the lymphatic system. Anaesth. Intensive Care Med. 2019, 20, 182–189.

(47). Collins DS; Kourtis LC; Thyagarajapuram NR; Sirkar R; Kapur S; Harrison MW; et al. Optimizing the Bioavailability of Subcutaneously Administered Biotherapeutics Through Mechanochemical Drivers. Pharm. Res. 2017, 34, 2000–2011. [PubMed: 28707164]

(48). McDonald TA; Zepeda ML; Tomlinson MJ; Bee WH; Ivens IA Subcutaneous administration of biotherapeutics: current experience in animal models. Curr. Opin. Mol. Ther. 2010, 12, 461–470. [PubMed: 20677097]

(49). Song JY; Larson NR; Thati S; Torres-Vazquez I; Martinez-Rivera N; Subelzu NJ; et al. Glatiramer acetate persists at the injection site and draining lymph nodes via electrostatically-induced aggregation. J. Controlled Release 2019, 293, 36–47.

(50). Bender C; Eichling S; Franzen L; Herzog V; Ickenstein LM; Jere D; et al. Evaluation of in vitro tools to predict the in vivo absorption of biopharmaceuticals following subcutaneous administration. J. Pharm. Sci. 2022, 111, 2514. [PubMed: 35429492]

(51). Pedregosa F; Varoquaux G; Gramfort A; Michel V; Thirion B; Grisel O; et al. Scikit-learn: Machine Learning in Python. J. Mach. Learn. Res. 2011, 12, 2825–2830.

(52). Chiang P-C; Nagapudi K; Fan PW; Liu J Investigation of Drug Delivery in Rats via Subcutaneous Injection: Case Study of Pharmacokinetic Modeling of Suspension Formulations. J. Pharm. Sci. 2019, 108, 109–119. [PubMed: 29909029]

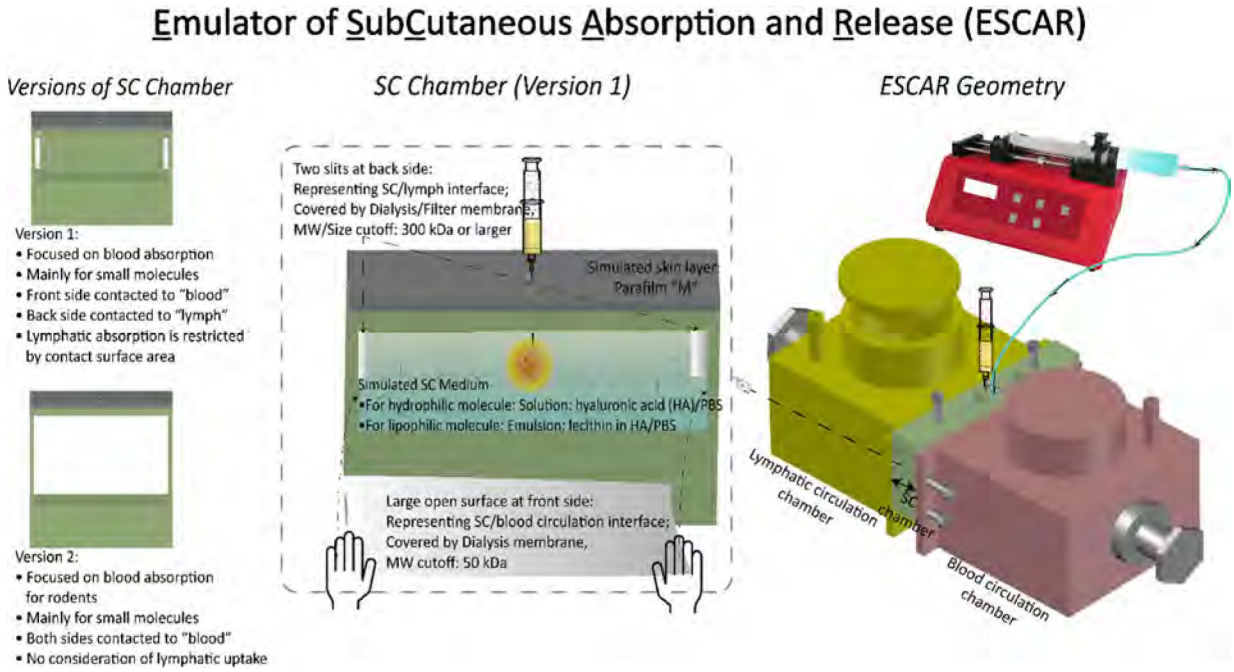

Figure 1. ESCAR design to emulate the in vivo SC environment.

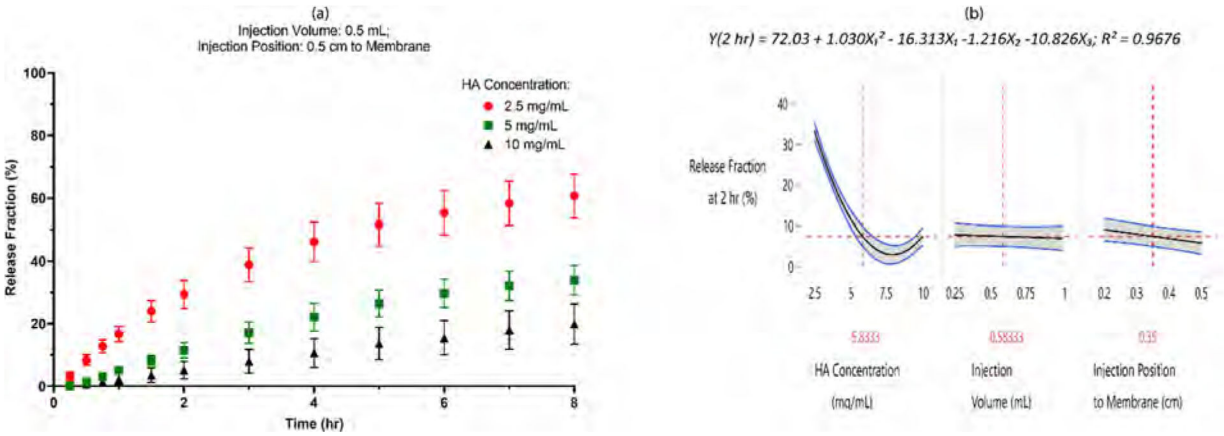

Figure 2. (a) In vitro release profile of acetaminophen; (b) prediction profiler plot of release friction (%) at 2 h.

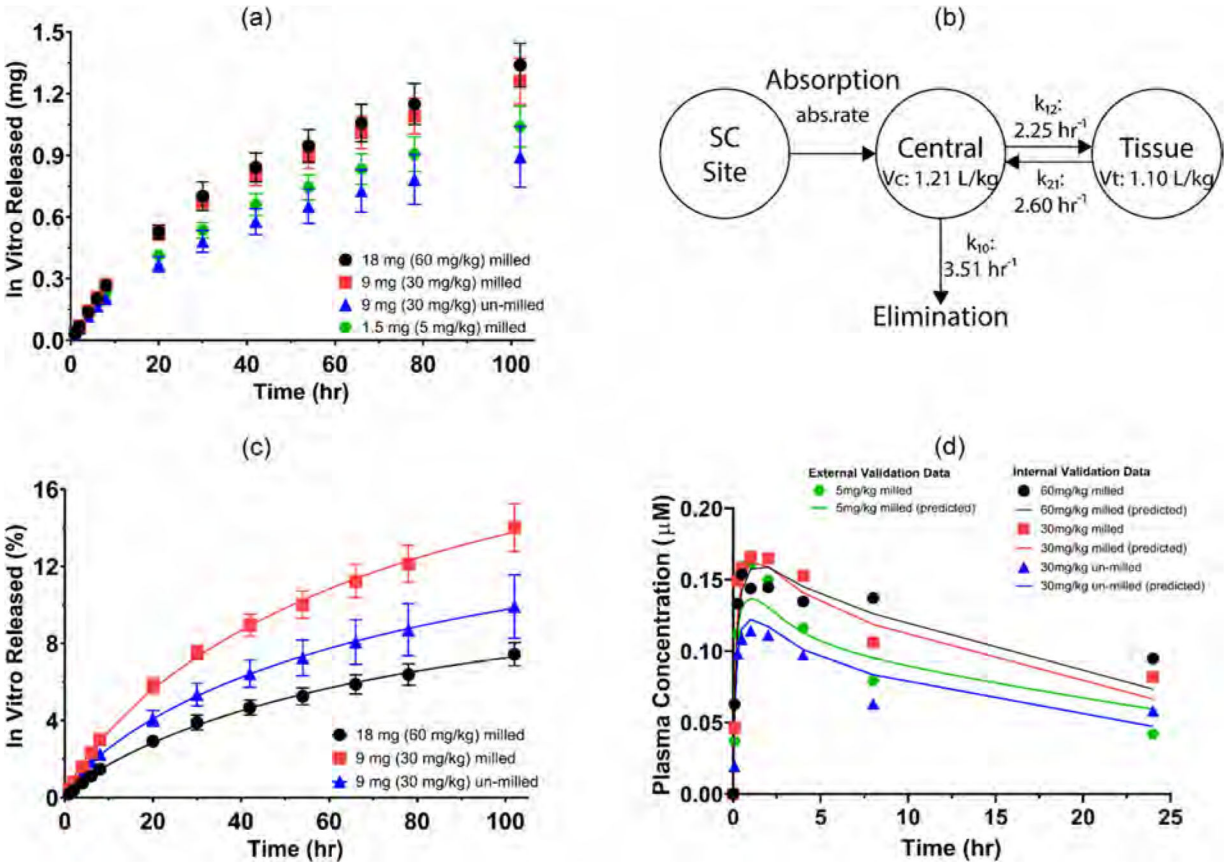

Figure 3.

IVIVC model development for griseofulvin suspensions: (a) in vitro release profile (mg); (b) PK model for the SC administration of griseofulvin; (c) in vitro release profile (%); and (d) predicted and experimental griseofulvin plasma concentration profiles.

Table 1.

Internal and External Validation for the IVIVC Model of Griseofulvin Suspensions

		C_{max} (μM)			AUC_{0-24} (μM X h)		
dose/formulation	**data type**	**obs.**	**pred.**	**%PE**	**obs.**	**pred.**	**%PE**
18 mg (60 mg/kg) milled	internal	0.154	0.163	−5.7	2.95	2.77	6.1
9 mg (30 mg/kg) milled	internal	0.166	0.165	0.9	2.64	2.63	0.5
9 mg (30 mg/kg) un-milled	internal	0.114	0.109	4.4	1.71	1.74	−2.2
average absolute %PE for internal validation				3.6			2.9
1.5 mg (5 mg/kg) milled	external	0.161	0.137	14.9	1.91	2.13	−11.5